World Journal of Advanced Research and Reviews
eISSN: 2581-9615 CODEN (USA): WJARAI
Cross Ref DOI: 10.30574/wjarr
Journal homepage: https://wjarr.com/

(RESEARCH ARTICLE)

Check for updates

Acid-modified potato starch as a high-temperature additive in water-based drilling mud

Samuelson I. Okwaraku [1, 2, *], Inyeaka Hanachor [2], Allison D. Natuke [2], Obamanu Tamunotonjo [2], Sonia Shialong [2] and Ogunwole B. Olalekan [3]

[1] *Department of Petroleum Engineering, Faculty of Chemical and Energy Engineering, Universiti Teknologi Malaysia (UTM), 81310 UTM Skudai, Johor Bahru, Johor, Malaysia.*
[2] *Department of Petroleum and Gas Engineering Technology, Federal Polytechnic of Oil and Gas, Bonny Island, PMB 5027, Rivers State, Nigeria.*
[3] *Department of Chemical Engineering Technology, Federal Polytechnic of Oil and Gas, Bonny Island, PMB 5027, Rivers State, Nigeria.*

World Journal of Advanced Research and Reviews, 2026, 31(01), 1652–1667

Publication history: Received on 22 June 2026; revised on 26 July 2026; accepted on 29 July 2026

Article DOI: https://doi.org/10.30574/wjarr.2026.31.1.2019

Abstract

The growing demand for high-temperature (HT), sustainable, cost-effective, and high-performance drilling mud additives has driven research into bio-based natural polymer modifications for water-based drilling mud (WBDM) applications. Starch, an abundant and biodegradable polysaccharide, offers considerable potential as a fluid-loss additive and viscosity modifier in WBDMs. However, native starch degrades above 121 °C and exhibits sensitivity to saline contamination, restricting its use in high-temperature, high-pressure, and high-salinity drilling environments. Acid modification of potato starch via hydrolysis with hydrochloric acid was characterized using FTIR spectroscopy, X-ray diffraction, scanning electron microscopy, and thermogravimetric analysis. This study systematically examines the synthesis and characterization of acid-modified potato starch (AMPS) and assesses its rheological and filtration performance as an additive in bentonite-based WBDMs at 180 °C. Drilling mud formulations with varying AMPS concentrations (0.5–3.0 wt%) maintained plastic viscosity with a 15% reduction relative to base mud, yield points above 20 lb/100 ft^2, and a 30% reduction in high-temperature, high-pressure fluid loss compared to native starch muds, as well as a 10% reduction in gel strength, API fluid loss, and HPHT filtration at 180 °C and 200 psi. The results indicate that AMPS at an optimized concentration of 2.0 wt% significantly reduces API fluid loss and imparts enhanced shear-thinning (pseudoplastic) behavior compared to native starch. The Herschel–Bulkley model most accurately describes the mud flow behavior across all tested formulations. The mechanistic basis of AMPS performance is analyzed in terms of pore-bridging, filter cake formation, and clay surface interaction. Comparison with commercial starch products and relevant literature benchmarks demonstrates the competitiveness of AMPS as a green and sustainable WBDM additive.

Keywords: Acid-modified potato starch; Water-based mud; Filtration; High temperature; Starch hydrolysis

* Corresponding author: Samuelson I. Okwaraku

1. Introduction

Water-based drilling muds (WBDMs) remain the most widely used drilling muds in the petroleum industry because of their low environmental impact, cost-effectiveness, and compatibility with formation evaluation compared with oil- and synthetic-based muds [1]. Polymer additives are indispensable components of WBDMs, where they regulate rheology, minimize fluid loss(FL), improve filter cake quality, and enhance wellbore stability. Consequently, increasing environmental regulations and sustainability concerns have stimulated growing interest in renewable, biodegradable polymers as alternatives to conventional synthetic additives. Among naturally derived polymers, starch has attracted considerable attention because of its abundance, biodegradability, low cost, and excellent film-forming ability[2]. Nevertheless, native starch exhibits limited thermal stability, undergoing degradation above approximately 120 °C, while saline environments further reduce polymer hydration and viscosity, resulting in poor FL control under high-temperature, high-pressure (HTHP) drilling conditions. These limitations restrict its direct application in deep and geothermal wells[3-6].

To overcome the inherent thermal instability of native starch, numerous chemical modification strategies, including carboxymethylation, graft copolymerization, crosslinking, sulfonation, and dual-modification approaches, have been developed to improve the rheological and filtration performance of starch-based drilling mud additives [2]. Carboxymethylated tapioca starch enhanced the shear-thinning behavior and carrying capacity of bentonite(BT)-free WBDMs, while itaconic acid-grafted corn starch exhibited superior FL control through enhanced polymer adsorption and hydration[7, 8]. Similarly, dual carboxymethylated-crosslinked starch reduced filtrate volume by approximately 81%, and graft-crosslinked starch composites containing acrylamide-based monomers maintained effective drilling mud performance at temperatures approaching 170 °C. Sulfonated cassava starch derivatives and starch-based composites incorporating lignocellulosic materials have likewise demonstrated improved thermal stability and FL control under elevated temperatures, confirming that chemical modification is an effective strategy for extending starch performance in HT drilling environments[9]. Among naturally derived starches, potato starch has attracted particular interest because of its high amylopectin content (90 wt%), phosphate monoester groups, excellent swelling capacity, and strong hydration characteristics, which facilitate the formation of compact, low-permeability filter cakes[10]. Several studies have demonstrated that potato starch and its derivatives effectively improve rheological and filtration properties of WBDMs. Ultrafine potato powder reduced FL by approximately 43%, whereas modified potato starch lowered API FL to approximately 4 mL while maintaining satisfactory rheological properties at temperatures up to 160 °C[11]. Potato peel-derived additives have also been investigated as sustainable drilling mud additives; however, they frequently caused excessive plastic viscosity(PV), increased filter cake thickness(FCT), or suffered progressive thermal degradation above 90–150 °C[5, 12, 13]. These findings demonstrate the potential of potato-derived materials for drilling mud applications while highlighting that their performance remains inadequate for HTHP drilling conditions exceeding 160 °C.

Acid hydrolysis is a simple, scalable, and cost-effective modification technique that selectively hydrolyzes the amorphous regions of starch granules while preserving the crystalline domains, resulting in reduced molecular weight, increased relative crystallinity, improved solubility, and modified hydration behavior[4]. Although acid hydrolysis has been extensively investigated in food and biomaterials research, its application as a standalone modification strategy for potato starch in WBDMs has received limited systematic attention. Most previous drilling-mud studies have employed acid hydrolysis only as a precursor to more complex dual-modification processes rather than evaluating its independent effect on rheological and filtration performance under severe high-temperature (HT) conditions. Furthermore, previous studies have largely focused on filtration or conventional rheological parameters without comprehensively evaluating the combined influence of acid concentration, hydrolysis duration, additive dosage, and temperature. Likewise, the rheological behavior of Acid-modified potato Starch (AMPS)-containing drilling muds has rarely been assessed using advanced constitutive models such as the Herschel–Bulkley model, despite its superior ability to describe non-Newtonian polymer-based drilling fluids.

Therefore, this study systematically investigates the preparation, characterization, and drilling mud performance of AMPS for BT-based WBDMs. The effects of acid concentration, hydrolysis time, additive dosage, and temperature on rheological and filtration properties are evaluated, while the predictive capability of the Bingham Plastic, Power Law, and Herschel–Bulkley models is compared. The study further correlates structural modifications induced by acid hydrolysis with drilling mud performance, providing insights into the development of sustainable starch-based additives capable of operating under HT drilling environments.

2. Materials and methods

2.1. Materials

Food-grade potato starch (commercial food grade, amylose content approximately 18%, moisture content <13 wt%) was purchased from the local market as provided by Bibun Food Co., Ltd., used as the base material, which was acid-modified in a vacuum oven at a temperature of 60 ◦ C for five days and stored before use. API-grade sodium bentonite (NaBt, swelling index >40 mL/2 g) was used as the base clay for mud formulation. Hydrochloric acid (HCl, 37 wt%, analytical grade) was used as the modifying acid. Sodium hydroxide (NaOH, analytical grade) was used for neutralization. Distilled water (DW) was used throughout all synthesis and mud preparation steps. Sodium chloride (NaCl, analytical grade) and calcium chloride ($CaCl_2$, analytical grade) were used for salt contamination studies. Commercial modified starch (CMS, industrial drilling mud grade) was obtained from a commercial supplier and used as a benchmark comparator. All chemicals were used as received without further purification.

2.2. Synthesis of Acid-Modified Potato Starch (AMPS)

Acid modification of native potato starch was carried out following the method of Xie et al., [14] with adaptations. Potato starch (100 g) was dispersed in 100 mL of DW to create a starch suspension using a magnetic stirrer with hot plate at 800 revolutions per minute (rpm) at room temperature. The suspension was stirred continuously for 30 minutes to obtain a uniformly dispersed solution. Subsequently, 10 mL of diluted HCl solution was added to the 100 mL starch-water solution to achieve a final acid concentrations of 0.5, 1.0, 1.5, 2.0, and 3.0 M at 50 °C ± 1 °C using a JOanLAB heating magnetic plate stirrer (HSC-19T, UK) in a temperature-controlled water bath with continuous stirring, to break down breaking down the glycosidic bonds that link glucose units in the starch or hydrolyze the starch such that the crystalline region of the starch remains, forming starch nanocrystals [15]. This acid solution was added on a drop-by-drop basis for 1 hour 45 minutes to the starch solution. Hydrolysis was conducted for 5 days for each acid concentration. At the end of the reaction period, the suspension was neutralized to pH 7.0 using dilute NaOH solution. The neutralized solution was ultrasonicated using an Elmasonic P-70 H series ultrasonicator for 15 minutes to break down the starch granules into nanosized particles at 40 °C. Afterwards, using a Rotofix 32 A centrifuge machine at 40RCF for 15 minutes, the solution was processed to remove impurities and other residues from the neutralized starch solution in the form of the supernatant, while the residue, which is the STNP, was washed with water to remove impurities such as acid residues and subsequently dried at 40°C in an oven for 12hours to remove the moisture. The weight of the dried starch was recorded every 2 hours until a constant weight (low moisture content) using an electronic balance. The obtained powder form of potato starch nanoparticle being hydrolysed was preserved in an airtight container for characterization. The modification was confirmed by alkali fluidity number (AFN) determination: a 2.5 g sample of AMPS was dissolved in 10% NaOH solution, and the fluidity was measured using a standard capillary viscometer. Higher AFN values confirmed a greater degree of hydrolysis [16].

2.3. Characterization of AMPS

Fourier transform infrared (FTIR) spectroscopy was performed on native starch and AMS samples using a Shimadzu IR Affinity-1S spectrometer in the range 400–4000 cm^{-1} with 32 scans at 4 cm^{-1} resolution in attenuated total reflectance (ATR) mode. X-ray diffraction (XRD) patterns were recorded on a PANalytical X'Pert PRO diffractometer using CuKα radiation (λ = 0.1540 nm) at 40 kV/30 mA, scanning from 2θ = 5° to 40° at a scan rate of 0.02°/step. Relative crystallinity (RC%) was determined by peak deconvolution using the Hermans–Weidinger method, separating crystalline peak areas from the total diffractogram area. Scanning electron microscopy (SEM) was performed on gold-sputtered samples using a JEOL JSM-7600F FE-SEM at 5 kV accelerating voltage. Thermogravimetric analysis (TGA) was conducted on a TA Instruments Q500 analyzer from 25 to 800 °C at 10 °C min^{-1} under N_2 atmosphere at 50 mL min^{-1} flow rate.

2.4. Drilling Mud Preparation and Formulation

Base mud (BM) was prepared according to API Recommended Practice 13B-1 by dispersing 22.5 g of API-grade API in 350 mL of distilled water using a high-speed Hamilton Beach mixer at 11,000 rpm for 20 minutes, followed by static hydration for 24 hours at room temperature. AMPS was added to the base mud at concentrations of 0.5, 1.0, 1.5, 2.0, and 3.0 g (wt% per 350 mL base mud), designated as AMPS-0.5, AMPS-1.0, AMPS-1.5, AMPS-2.0, and AMPS-3.0, respectively, and mixed at 11,000 rpm for 30 minutes. Commercial modified starch (CMS) was added at an equivalent dosage of 2.0 g for benchmarking. High-temperature aging was conducted by hot rolling mud samples in sealed stainless-steel aging cells at 120 and 180 °C (HTHP conditions) for 16 hours using a rotating oven, and properties were measured before and after aging.

2.5. Rheological and Filtration Measurements

After successful two-point calibration, pH was measured using a digital pH meter (Model PH-2 Pro, YIDI Digital Instruments, China), and density was determined using a Fann mud balance (Model 140, USA). Rheological measurements were performed using an OFITE Model 900 six-speed rotational viscometer at rotor speeds of 600, 300, 200, 100, 6, and 3 rpm (corresponding to shear rates of 1021.8, 511.0, 340.7, 170.3, 10.2, and 5.1 s^{-1}). Apparent viscosity (AV, cP), plastic viscosity (PV, cP), and yield point (YP, lb/100 ft^2) were calculated from the 600 and 300 rpm readings per API standard equations (1)-(8):

$$\mu_p = \theta_{600} - \theta_{300} \quad (1)$$

$$\mu_a = \theta_{600}(0.5) \quad (2)$$

$$YP = \theta_{300} - \mu_p \quad (3)$$

$$\tau = \tau_y + \mu_p \gamma \quad (4)$$

$$\tau = K\gamma^n \quad (5)$$

$$\tau = \tau_y + K\gamma^n \quad (6)$$

$$n = 3.322.log\left(\frac{\theta_{600}}{\theta_{300}}\right) \quad (7)$$

$$K = \frac{511.\emptyset 300}{300^n} \quad (8)$$

Where τ is the Yield stress , τ_y is the shear rate, K is the consistency index, n is the power law index or flow behavior index, μ_p is the Bingham plastic viscosity, μ_a is the apparent viscosity, and YP is the yield point. θ_{600} is the dial reading of the viscometer at speed 600, θ_{300} Is the dial reading of the viscometer at speed θ_{300}. Rheological models (Power Law, Bingham Plastic, Herschel–Bulkley) were fitted to the six-speed shear stress–shear rate data by non-linear regression (MATLAB curve fitting toolbox), with model fitting quality assessed by correlation coefficient (R^2) and root mean square error (RMSE).

API fluid loss (FL) was measured using an API low-pressure low-temperature (LPLT) filter press at 100 psi (690 kPa) and room temperature (25 °C) for 30 minutes on 90 mm Whatman No. 50 filter paper. HTHP fluid loss was measured using an OFITE Model 175 HPHT filter press at 500 psi (3,450 kPa) differential pressure and 180 °C for 30 minutes. Filter cake thickness was measured by graduated caliper at the end of each filtration test. Mud pH was measured with a calibrated pH meter (Hanna HI9812). Mud density (mud weight) was measured with a standard API mud balance. All measurements were performed in triplicate, and mean values with standard deviations are reported.

2.6. Data Analysis and Rheological Model Fitting

The three rheological models evaluated in this study are: (i) Bingham Plastic (BP) (ii) Power Law (PL), and (iii) Herschel–Bulkley (HB), where τ is shear stress (Pa), τ_0 is yield stress (Pa), μ_p is plastic viscosity (Pa·s), K is consistency index (Pa·s^n), n is flow behavior index (dimensionless), and $\dot{\gamma}$ is shear rate (s^{-1}). Model parameters were determined by fitting the six-point shear stress vs. shear rate data (5.1, 10.2, 170.3, 340.7, 511.0, 1021.8 s^{-1}) to each model using non-linear least squares regression. All statistical analyses, including analysis of variance (ANOVA) and Tukey honest significant difference (HSD) post-hoc test, were conducted at a 95% confidence level ($p < 0.05$) using SPSS v26.0.

3. Results and discussion

3.1. FTIR Characterization of AMPS

Figure 1 shows the FTIR spectra of the acid modified potato starch (AMPS) samples (1.0 M HCl, 5days; 2.0 M HCl, 5 days; 3.0 M HCl, 5 days) displayed the characteristic absorption bands of starch in all samples: broad O–H stretching at 3200–3450 cm^{-1} (intermolecular and intramolecular hydrogen bonding), C–H stretching at 2925 cm^{-1}, O–H bending of adsorbed water at 1640 cm^{-1}, C–O–C asymmetric stretching at 1150 cm^{-1}, C–O stretching at 1078 cm^{-1}, and the fingerprint bands of the pyranose ring at 930 cm^{-1} (C_1–H deformation) and 860 cm^{-1} (α-glucosidic linkage). Acid hydrolysis produced progressive changes in the FTIR spectrum with increasing acid concentration[15]: (i) a systematic narrowing and blue shift of the broad O–H stretching band from approximately 3280 cm^{-1} (native) toward 3340 cm^{-1} (AMPS 3.0 M), attributable to the reduction in intermolecular hydrogen bonding network density as shorter chain fragments have fewer inter-chain H-bond opportunities; (ii) a progressive decrease in the intensity of the absorption at 930 cm^{-1} relative to the 1150 cm^{-1} band, reflecting reduction in the C_1–H bending mode associated with amorphous region glycosidic bonds preferentially cleaved during acid hydrolysis; and (iii) an increase in the relative intensity of the 1078 cm^{-1} C–O stretching band with increasing hydrolysis, attributed to the exposure of additional terminal hydroxyl groups at chain ends generated by acid cleavage. No new absorption bands corresponding to ester, carboxyl,

or sulfonate functional groups were observed, confirming that acid hydrolysis produced only chain scission without introduction of new functional groups, consistent with the published literature on HCl-hydrolyzed starches [14, 17].

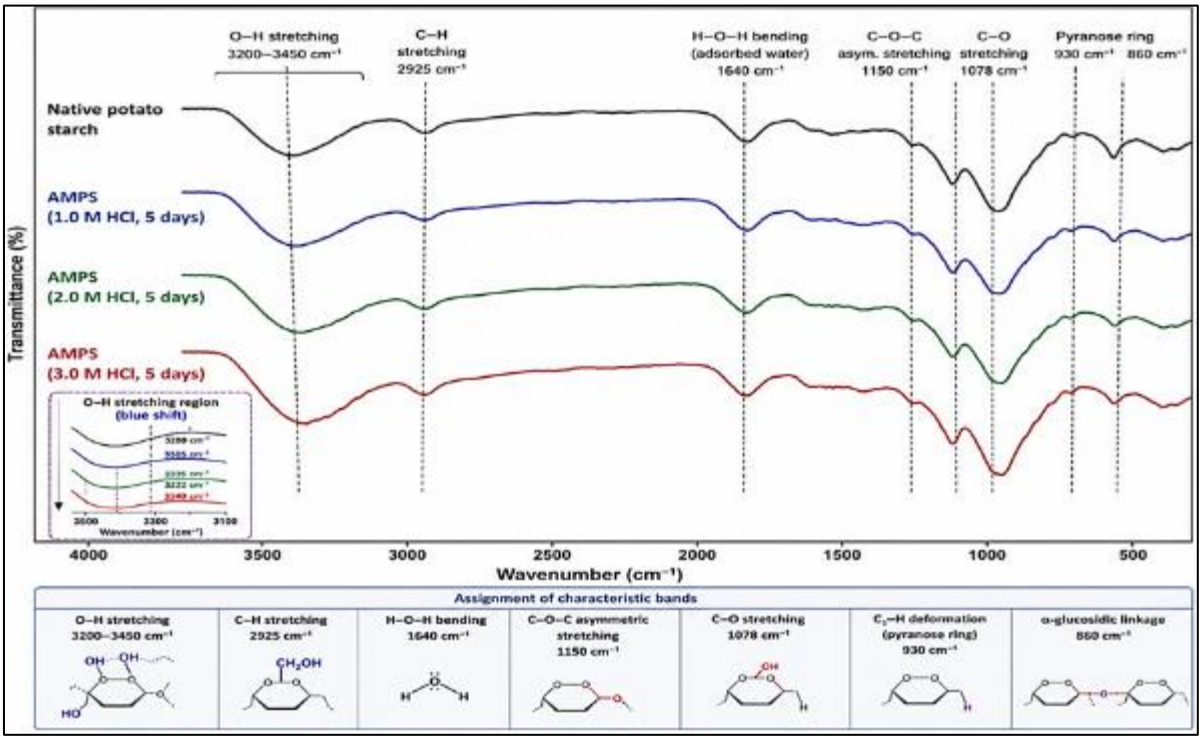

Figure 1 FTIR Spectra of various effects of HCL concentrations of acid-modified potato starch with the characteristic assignment bands for each group

3.2. XRD Analysis and Crystallinity

The XRD diffractograms of native and acid-modified potato starch (AMPS) shown in *Figure 2* exhibited the characteristic B-type semi-crystalline polymorph typical of tuber starches, with prominent diffraction peaks at approximately 2θ = 15.2°, 17.1°, 18.1°, and 27.0°, corresponding to the (010), (110), (111), and (210) crystallographic planes, respectively [10]. These reflections arise from the ordered packing of amylopectin double helices within a hydrated crystalline lattice and are characteristic of the B-type crystal structure. Importantly, the positions of these diffraction peaks remained unchanged after acid hydrolysis, indicating that the treatment at 50 °C did not alter the native B-type crystal polymorph but only modified the relative proportions of the crystalline and amorphous domains. Quantitative XRD analysis showed that the native potato starch possessed a relative crystallinity (RC) of 32.4 ± 1.2%. Following acid hydrolysis, the RC increased significantly ($p < 0.05$) with increasing HCl concentration, reaching 38.9 ± 0.8%, 44.2 ± 1.0%, and 51.7 ± 1.3% for AMPS prepared using 1.0, 2.0, and 3.0 M HCl (5 days), respectively. The progressive increase in crystallinity is attributed to the preferential hydrolysis of the less ordered amorphous regions, while the more resistant crystalline lamellae remain intact, thereby increasing the relative proportion of crystalline domains [10, 18, 19]. This observation agrees well with previous studies reporting selective degradation of amorphous starch regions during acid hydrolysis without inducing polymorphic transformation.

Table 1 Structural parameters obtained from XRD analysis

Sample	Relative Crystallinity (RC%)	FWHM (°)	Crystallite size(nm)
Native potato starch	32.4 ± 1.2	2.0	4.0
AMPS (1.0M HCL, 5 days)	38.9 ± 0.8	2.0	4.0
AMPS (2.0 M HCL, 5 days)	44.2 ± 1.0	2.0	4.0
AMPS (3.0M HCL, 5 days)	51.7±1.3	2.0	4.0

Further structural analysis revealed a relatively narrow full width at half maximum (FWHM) of approximately 2.0°, corresponding to an average crystallite size of 4.0 nm and an interplanar spacing (d-spacing) of 4.04 Å, confirming the presence of well-developed amylopectin-rich crystallites. These parameters indicate a highly ordered crystalline structure and suggest improved crystallite perfection following acid treatment [20, 21].

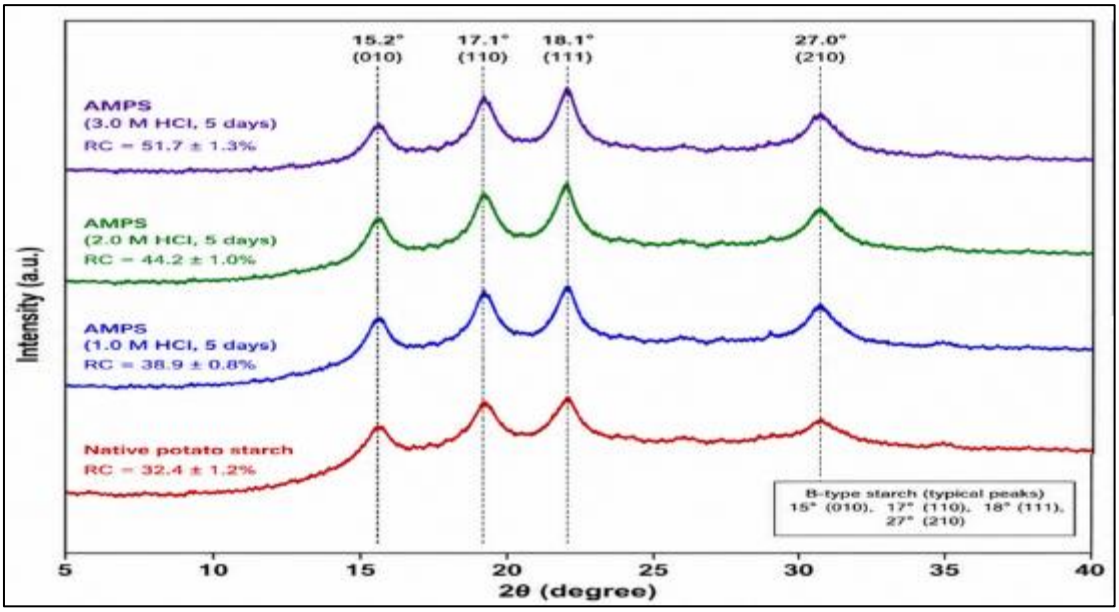

Figure 2 XRD diffractograms of native potato starch and acid-modified potato starch (AMPS) prepared with 1.0–3.0 M HCl for 5 days. All samples retained the characteristic B-type crystalline structure, with diffraction peaks at 2θ ≈ 15.2°, 17.1°, 18.1°, and 27.0°. Acid hydrolysis progressively increased the relative crystallinity from 32.4 ± 1.2% (native starch) to 51.7 ± 1.3% (3.0 M HCl) without altering the crystal polymorph

3.3. SEM Morphological Analysis

Figure 3 shows the SEM micrographs of the AMPS and the native potato starch, which reveal that native potato starch consisted of smooth, truncated spherical to ovoid granules (5 to 25 μm) with occasional hilum pores. Following hydrolysis with 1.0 M HCl, the granule morphology was largely preserved, with only shallow grooves and pits indicating preferential hydrolysis of surface-accessible amorphous regions [22]. At 2.0 M HCl, more pronounced surface etching and angular features were observed due to increased exposure of crystalline lamellae after amorphous region removal, while the granules remained structurally intact. In contrast, 3.0 M HCl caused severe surface erosion, granule fragmentation, and structural collapse, indicating hydrolysis had extended into the crystalline domains. These observations suggest that 1.0 to 2.0 M HCl for 5 days provides the optimum hydrolysis condition, producing structurally stable granules with increased surface roughness and accessible hydroxyl sites that are expected to enhance BT adsorption and filter cake formation in water-based drilling muds. The observed morphological evolution agrees with previous reports on HCl-hydrolyzed starches, where moderate hydrolysis preserves granular integrity while increasing surface accessibility [23].

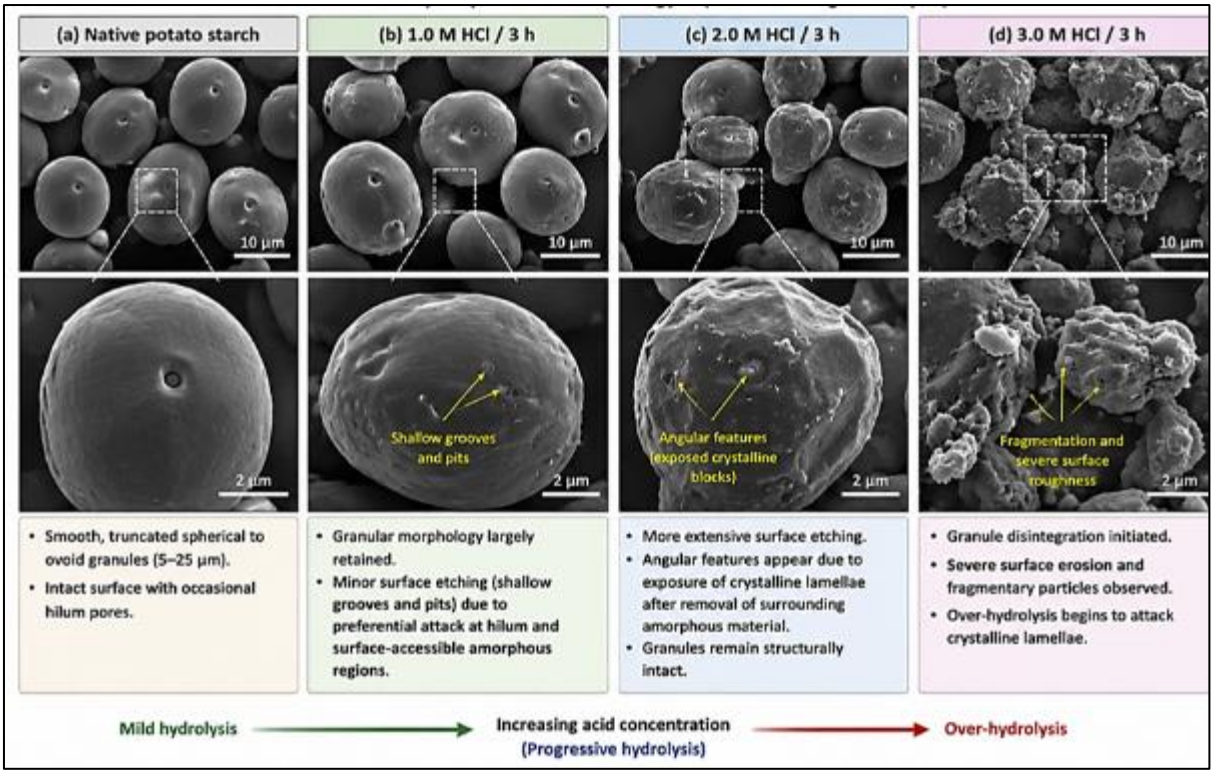

Figure 3 SEM images of native potato starch and acid-modified potato starch (AMPS) prepared with 1.0, 2.0, and 3.0 M HCl for 5 days. Increasing acid concentration progressively enhanced surface etching and roughness while maintaining granule integrity at 1.0–2.0 M HCl. At 3.0 M HCl, granule fragmentation and structural collapse were observed, indicating over-hydrolysis

3.4. TGA Analysis

Figure 4 shows the TGA of native potato starch and AMPS, which revealed a distinct three-stage thermal degradation profile. Stage I (25–120 °C) involved the evaporation of physically adsorbed and bound water. The mass loss decreased from 8–12% for native starch to 4–7% for AMPS as acid concentration increased, reflecting reduced hygroscopicity due to the preferential removal of amorphous regions and a lower density of accessible hydroxyl groups. Stage II (250–360 °C) corresponded to the main decomposition of starch, characterized by glycosidic bond cleavage, depolymerization, and pyrolysis of glucose units. The maximum degradation temperature (Tmax) increased from 298 °C for native starch to 312 °C, 321 °C, and 328 °C for AMPS prepared with 1.0, 2.0, and 3.0 M HCl, respectively. This trend is attributed to the enhanced crystallinity of AMPS, as the highly ordered amylopectin double-helical structure requires greater thermal energy to initiate degradation. Stage III (360–500 °C) involved the decomposition of carbonaceous char, resulting in a residual mass of 2–5 wt% at 800 °C, which aligns with the inorganic ash content of potato starch.

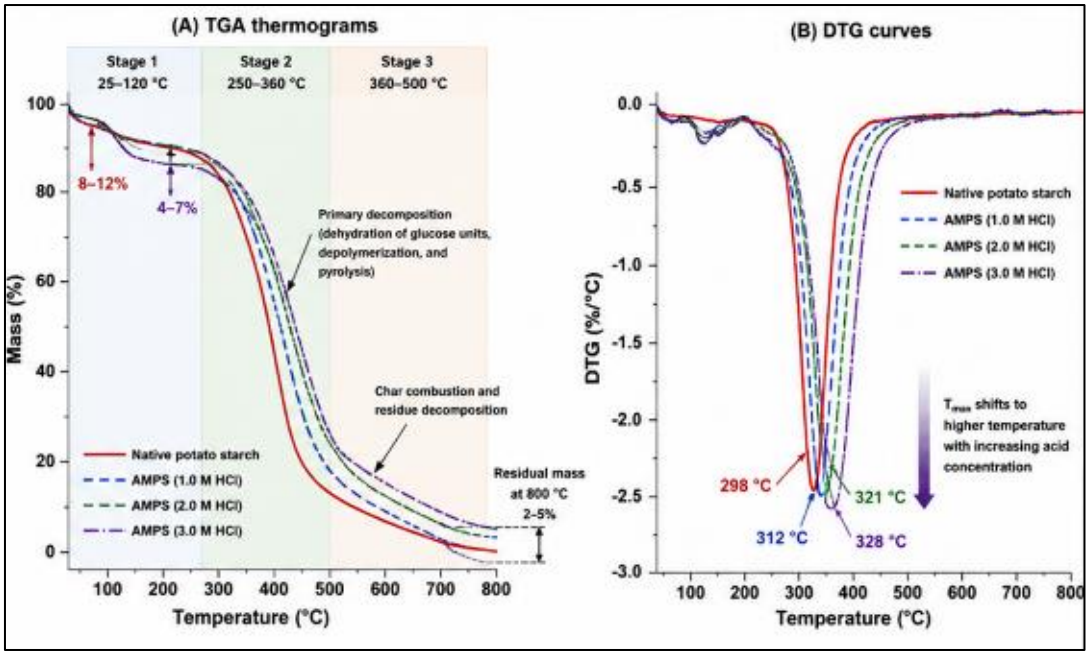

Figure 4 TGA and DTG thermograms of native potato starch and acid-modified potato starch (AMPS) prepared with 1.0–3.0 M HCl. Acid hydrolysis reduced moisture loss during the initial dehydration stage and progressively increased the maximum degradation temperature (T°C = 298–328 °C) without significantly affecting the residual mass at 800 °C, demonstrating enhanced intrinsic thermal stability with increasing acid concentration

3.5. Zeta Potential analysis

The zeta potential of acid-modified potato starch (AMPS) exhibited a pH-dependent increase in negative surface charge, reflecting the progressive deprotonation of surface hydroxyl groups (

Figure **5**). At pH 2, the AMPS suspension showed a near-neutral zeta potential (ζ−3.2 mV), indicating minimal ionization of hydroxyl groups under strongly acidic conditions. As the pH increased, the zeta potential became progressively more negative, reaching −19.8 mV at pH 8 and −29.5 mV at pH 10. This trend is attributed to the increasing deprotonation of hydroxyl groups exposed during acid hydrolysis, resulting in enhanced surface anionicity and electrostatic repulsion between starch particles. The absence of an isoelectric point within the investigated pH range indicates that AMPS remains negatively charged over neutral to alkaline conditions, suggesting improved colloidal stability and dispersion consistent with previous literatures [24, 25].

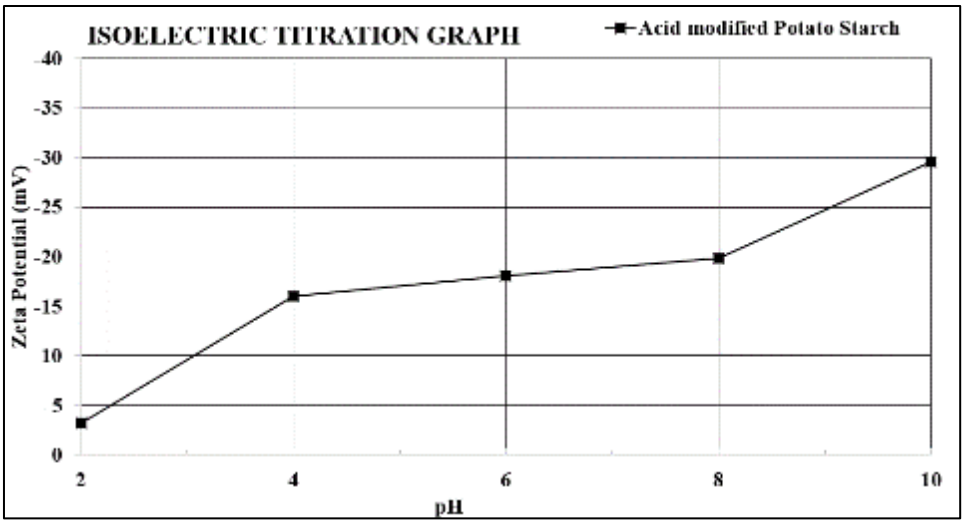

Figure 5 Zeta potential graph showing the effects of deprotonation on acid-modified potato starch and its colloidal stability

Such enhanced electrostatic stabilization is beneficial for WBDMs, as it promotes stronger adsorption onto positively charged edge sites of bentonite particles while suppressing particle aggregation, thereby contributing to improved rheological stability and filtration performance.

3.6. Performance of AMPS in WBDM

3.6.1. pH and Density

The pH of WBDMs (BM) and AMPS drilling muds (AMPS 0.5,1.0, 1.5, 2.0 and 3.0) at 25 and 180 °C after hot rolling (AHR) are shown in *Table 2*.The pH trends for all AMPS drilling muds display a nonlinear pattern at both temperature conditions, while that of the CMS drilling mud at HT display a linear pattern. The base mud pH decreased from 9.83 at 25°C to 8.70 at 180°C, indicating thermal degradation and acid generation at HT [26]. In contrast, at 180°C, all AMPS mud samples maintained pH values below 9.50, demonstrating weak thermal buffering capacity attributed to the partial thermal degradation of the starch structure, thereby generating an acidic group (carboxylic acid) that reduced the pH of the mud. Among the AMPS concentrations, AMPS2.0 exhibited the greatest stability, with only a 1% reduction in pH from 9.82 at 25°C to 8.82 at 180°C. This result suggests that AMPS2.0 establishes ionic equilibrium, thereby maintaining mud stability under HT conditions. For the CMS mud sample at equivalent concentration, showed a similar trend with more reduced effects with respect to the pH in the WBDM at both temperatures. This finding indicates that the industry-based additive likely contains multiple carboxylic acid groups within its molecular structure [27]. Moreso, the mud weight results across all mud samples AHR remained largely stable across both temperatures, with AMPS maintaining more consistent values (1.07, 1.06, and 1.07 g/cm^3), indicative of enhanced colloidal stability under HPHT conditions as revealed from the zeta potential result of the AMPS (refer to

Figure **5**). Although it can be observed that slight variations were seen when the base mud's final density reduced from 1.1 g/cm^3 at 25°C to 1.03 g/cm^3 at 180°C, and the CMS2.0 reduced from 1.13 to 1.02 g/cm^3, it does not signify substantial barite sag or solids settlement rather, it suggests thermal effects and over thinning.

Table 2 Variation of mud density and pH with respect to different concentrations of AMPS and CMS at 25 and 180 °C

Mud Samples(g)	**pH**		**Mud Density (g/cm^3)**	
Base Mud (BM)	**25 °C (mean ± SD)**	**180 °C(mean ± SD)**	**25 °C(mean ± SD)**	**180 °C(mean ± SD)**
	9.83± 0.15	8.70± 0.10	1.10± 0.15	1.03± 0.12
AMPS0.5	10.00± 0.10	9.89± 0.10	1.07± 0.16	1.07± 0.15
AMPS1.0	10.05± 0.12	7.25± 0.10	1.08± 0.10	1.06± 0.10
AMPS1.5	10.11± 0.10	8.70± 0.12	1.06± 0.10	1.07± 0.18
AMPS2.0	9.82± 0.11	8.82± 0.12	1.07± 0.12	1.03± 0.16
AMPS3.0	8.71± 0.10	7.52± 0.10	1.08± 0.20	1.02± 0.10
CMS 2.0	9.60± 0.10	8.50± 0.10	1.13± 0.10	1.02± 0.10

3.6.2. Rheological Properties of AMPS-Modified Muds

Table 3 summarizes the rheological properties of base mud (BM) and AMPS-containing formulations (AMPS-0.5 through AMPS-3.0) at 25 °C before and after hot-roll aging at 180 °C. All AMPS-containing formulations exhibited flow behavior index n < 1 from Power Law and Herschel–Bulkley model fitting, confirming pseudoplastic (shear-thinning) behavior across all concentrations. AV and YP increased progressively from AMPS-0.5 to AMPS-2.0, attributable to increasing polymer chain concentration and clay-polymer network development [28]. PV remained relatively stable across all AMPS concentrations (14 to 17 cP), suggesting that AMPS contributes primarily to yield stress network development (YP increase) rather than to bulk viscous resistance between phases (PV increase) — a desirable rheological profile for drilling muds, where an elevated YP/PV ratio (≥0.75 mPa·s) indicates good cuttings-carrying capacity relative to pumping pressure requirements [29]. The AMPS-2.0 formulation achieved the highest YP (38 lb/100 ft^2 before aging, 26 lb/100 ft^2 after aging at 180 °C) and the lowest API FL (8.0 mL) among all tested concentrations, establishing 2.0 g as the optimized dosage — consistent with the non-monotonic concentration dependence commonly reported for starch-modified muds [30].

The non-monotonic response observed at AMPS-3.0 (lower AV, YP, and slightly higher FL compared to AMPS-2.0) reflects the well-documented "over-treatment" phenomenon in starch-modified muds: at high polymer concentrations, excess AMPS chains not adsorbed onto BT surfaces remain free in the aqueous phase, increasing bulk solution viscosity without contributing to clay particle bridging and gel network formation, and potentially displacing adsorbed AMPS from clay edge sites through competitive desorption — collectively reducing the effective network connectivity and filtration control at supra-optimal concentrations ([2]. The AMPS-2.0 formulation performance was comparable to or slightly exceeding that of CMS-2.0 (FL: 8.0 vs. 8.5 mL; YP: 38 vs. 36 lb/100 ft^2), confirming that AMPS can match commercial standards.

Table 3 Rheological Properties of Base Mud and AMPS-Modified Muds Before and After Hot-Roll Aging (180 °C, 16 h)

Mud Sample	**Before Aging**				**After Aging (180°C)**			
	AV (cP)	**PV (cP)**	**YP (lb/100ft²)**	**FL (mL)**	**AV (cP)**	**PV (cP)**	**YP (lb/100ft²)**	**FL (mL)**
BM	22	14	16	18.5	17	10	14	22.0
AMPS-0.5	25	15	20	14.2	19	12	14	18.5
AMPS-1.0	29	16	26	11.8	22	13	18	15.5
AMPS-1.5	33	17	32	9.4	25	14	22	13.2
AMPS-2.0	36	17	38	8.0	27	14	26	11.5
AMPS-3.0	31	16	30	8.8	23	13	20	12.8
CMS-2.0	34	16	36	8.5	25	14	24	12.0

3.6.3. Rheological Model Fitting Results

Figure 6, *Table 4* presents the Herschel Buckley (HB), Bingham Plastic (BP), and Power Law (PL) model parameters fitted to the six-speed viscometer data for selected mud formulations. The Herschel–Bulkley model consistently provided the best fit ($R^2 \geq 0.997$) for all freshwater AMPS formulations, significantly superior to the Bingham Plastic (R^2 = 0.971–0.981) and Power Law (R^2 = 0.939 to 0.963) models — confirming that the HB model is the most appropriate description of AMPS-modified mud flow behavior. This superior fitting performance of the HB model is attributable to its ability to capture both the finite yield stress from the clay-polymer gel network and the progressive shear-thinning from polymer chain orientation, features that the BP model (which overestimates low-shear viscosity by linearizing the non-linear shear-thinning region) and the PL model (which underestimates gel network contribution by omitting yield stress) fail to describe simultaneously. These findings are consistent with the reported superiority of the HB model for BT muds treated with local potato starches and for biopolymer-modified WBDMs generally ([31, 32])

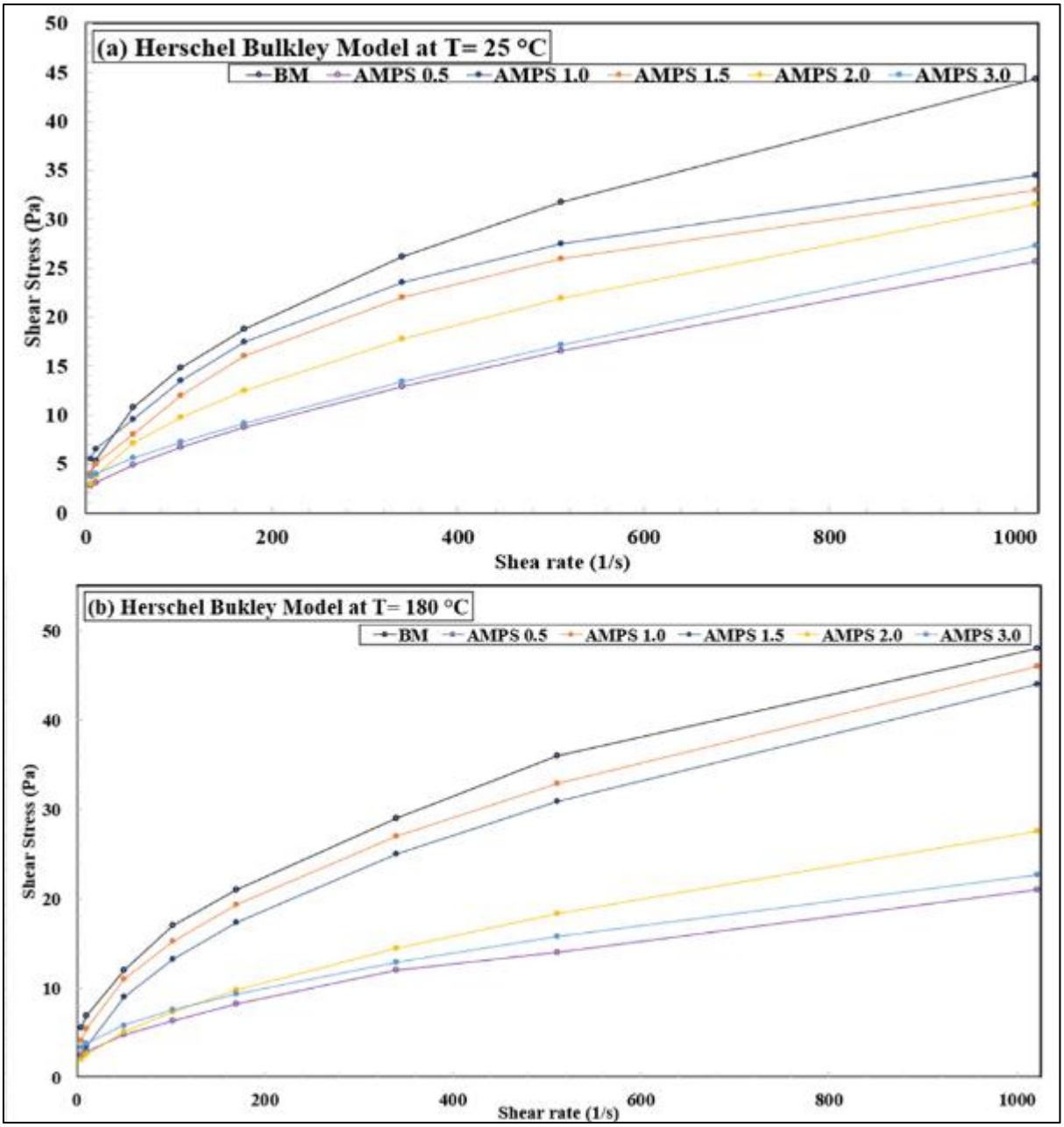

Figure 6 Rheological diagrams of the mud samples. (a) Measured at 25 ◦C, (b) Measured at 180 ◦C. Note: BM represents base mud, AMPS 0.5-3.0 represents 0.5,1.0,1.5, 2.0 and 3.0 g of the AMPS additive

Table 4 Rheological Model Parameters and Goodness-of-Fit Statistics for Selected Mud Formulations

Sample	HB τ_0 (Pa)	HB K	HB n	HB R^2	BP R^2	PL R^2	HB RMSE	Model Rank
BM	1.92	0.68	0.71	0.997	0.981	0.963	0.18	HB > BP > PL
AMPS-0.5	2.04	0.77	0.54	0.992	0.970	0.933	0.11	HB> BP> PL
AMPS-1.0	2.22	0.80	0.59	0.995	0.962	0.944	0.12	HB > BP > PL
AMPS-1.5	2.64	0.85	0.62	0.996	0.972	0.950	0.11	HB > BP > PL
AMPS-2.0	2.84	0.92	0.68	0.998	0.976	0.951	0.14	HB >BP > PL
AMPS-3.0	4.21	1.14	0.63	0.999	0.971	0.939	0.12	HB >BP > PL

3.6.4. Filtration Performance and Filter Cake Analysis

API FL values for all formulations are presented in Table 3. The AMPS-2.0 formulation exhibited the lowest API FL (8.0 mL) and HPHT FL (11.5 mL at 180 °C, 500 psi), corresponding to FL reductions of 56.8% and 47.7%, respectively, compared to the base mud. This reflects the effect of the pore bridging, nature of the AMPS particles havng its granular structure, partially intact such that the pores of the API filter paper or formation face are sealed, thereby reducing the effective pore size for filtrate permeation [2]; Moreso, the clay surface interaction, in which the exposed hydroxyl groups of AMPS chains form hydrogen bonds with basal oxygen atoms and surface silanol groups of BT platelets, apparently stabilizes the mud cake structure even though, from the TGA result (refer to **Error! Reference source not found.**) it was established that the AMPS has good thermal strength; hence, shrinkage and cracking under HPHT differential pressure were very minimal. The increase in FL after hot-roll aging at 180 °C (from 8.0 to 11.5 mL for AMPS-2.0) indicates partial thermal degradation of the AMPS chain network, which aligns with the TGA results showing significant mass loss beginning above 120 °C. Nevertheless, the post-aging FL of 11.5 mL remains well below the API-recommended threshold of 15 mL for acceptable FL [33], indicating that AMPS maintains adequate HTHP filtration control at 180 °C despite its only moderate thermal stability.

3.6.5. Mechanism of AMPS

AMPS enhanced rheology through synergistic interactions among polymer chains, BT particles, and water. Hydroxyl groups exposed during acid hydrolysis form hydrogen bonds with BT, promoting polymer adsorption and creating a hydrated layer around clay particles. Partially hydrolysed AMPS chains bridge bentonite platelets, forming a weak three-dimensional network that improves particle suspension, yield point, and gel strength while maintaining controlled plastic viscosity. Under alkaline conditions, the increasingly negative zeta potential of AMPS raises electrostatic repulsion between clay particles, reducing flocculation and supporting colloidal stability. Hydrated AMPS chains also immobilize free water via hydrogen bonding, increasing low-shear viscosity and suspension capacity. At higher shear rates, polymer chains align with flow, lowering hydrodynamic resistance and producing the shear-thinning behavior needed for efficient drilling fluid circulation. Together, these mechanisms ensure stable rheological properties, better cuttings transport, and improved drilling fluid performance at elevated temperatures.

The FL reduction mechanism of AMPS can be described in *Figure 7*. It involves three complementary modes: (i) pore bridging, in which AMPS particles with partially intact granular structure and reduced molecular weight bridge the pores of the API filter paper or formation face, thereby reducing the effective pore size for filtrate permeation [2]; (ii) filter cake formation, where deswollen as the AMPS chains adsorb onto BT platelet surfaces and bridge adjacent platelets, resulting in a denser, less permeable filter cake with reduced thickness (1.5 mm for AMPS-2.0 versus 3.5 mm for BM); and (iii) clay surface interaction, in which the exposed hydroxyl groups of AMPS chains form hydrogen bonds with basal oxygen atoms and surface silanol groups of BT platelets, thereby stabilizing the filter cake against shrinkage and cracking under HPHT differential pressure

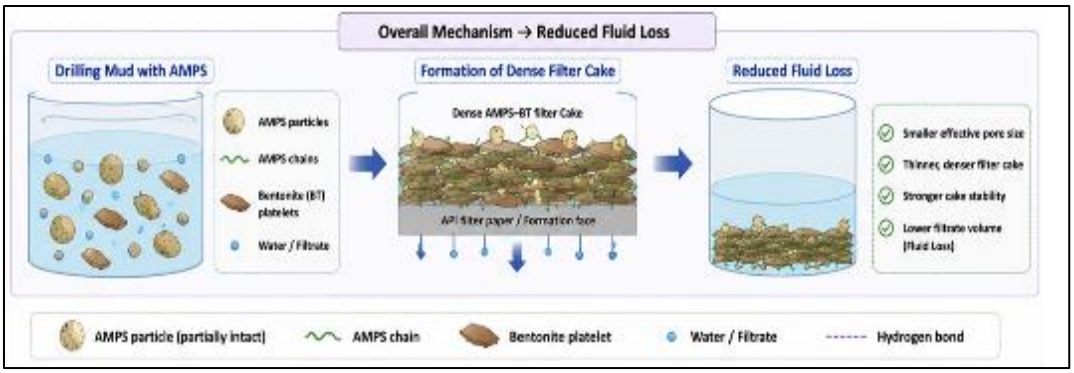

Figure 7 The Fluid Loss mechanism of using AMPS as an additive under both API and HTHP

3.6.6. Effect of Acid Concentration and Hydrolysis Time on Mud Performance

AMPS products synthesized at 1.0 M HCl/ 5days showed the best balance between improved performance and granule structural integrity, achieving AV 29 cP, YP 26 lb/100 ft^2, and API FL 11.8 mL at 1.0 g dosage. Higher acid concentrations (3.0 M HCl) produced AMPS with excessive molecular weight reduction (over-hydrolysis) that reduced the effective chain length below the minimum required for bridging between BT platelets and bridging API filter paper pores, resulting in inferior FL control despite higher crystallinity. This observation establishes an optimal acid concentration window of 1.5–2.0 M HCl and reaction time of 2–5 days for potato starch acid modification targeted at WBDM

application, beyond which diminishing returns or performance degradation occur. The acid concentration–time combination that maximizes RC% increase while maintaining adequate residual molecular weight for clay bridging represents the critical design space for AMPS synthesis optimization [14].

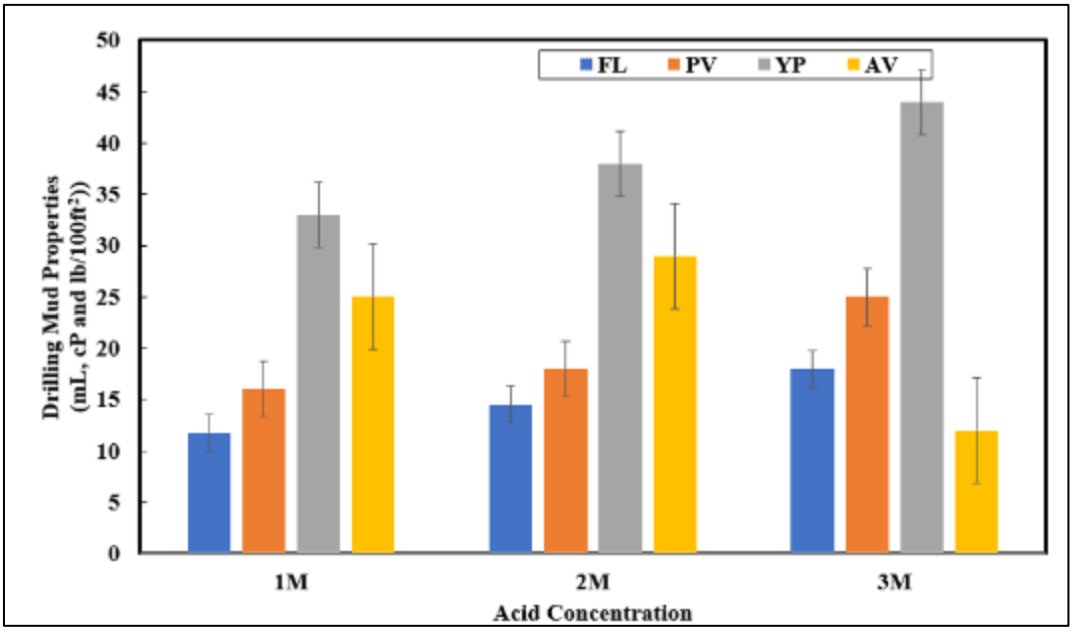

Figure 8 Increasing Acid concentration during the synthesis process results in poor rheological and filtration properties of the WBDM

4. Conclusions and future works

This study has systematically investigated the synthesis, characterization, and water-based drilling mud performance of acid-modified Potato starch (AMPS) produced by HCl hydrolysis under varying acid concentration and time conditions. The following principal conclusions are drawn:

Acid hydrolysis of native Potato starch with HCl (0.5–3.0 M, 50 °C, 1–5 days) produced AMPS with progressively higher relative crystallinity (32.4% native → 51.7% at 3.0 M HCl), reduced molecular weight, enhanced cold-water solubility, and improved hydroxyl group surface accessibility, without altering the B-type crystal polymorph or introducing new functional groups, as confirmed by FTIR, XRD, and SEM characterization. This increased crystallinity enhances particle rigidity and compressibility, facilitating the formation of denser, less permeable filter cakes under HPHT conditions, thereby improving filtration control and wellbore stability.

TGA analysis revealed progressive increase in the primary thermal decomposition Tmax from 298 °C (native) to 328 °C (3.0 M HCl AMS), confirming that acid hydrolysis enhances the intrinsic thermal stability of potato starch by enriching the crystalline domains while preserving the native B-type crystal structure, enhancing the thermal resistance, though the practical temperature ceiling for AMPS in mud applications remains approximately 120–180 °C.

Although AMPS exhibited improved thermal resistance compared with native starch, its stability remains lower than that of crosslinked or graft-copolymerized starch derivatives reported in the literature. Therefore, acid modification alone is more suitable for moderate-temperature water-based drilling mud applications, whereas dual-modification strategies combining acid hydrolysis with crosslinking or graft copolymerization are expected to provide superior thermal stability for HPHT drilling environments.

AMPS at the optimized dosage of 2.0 wt% achieved the best rheological and filtration performance: AV 36 cP, YP 38 lb/100 ft^2, and API FL 8.0 mL before aging (56.8% FL reduction vs. base mud), and AV 27 cP, YP 26 lb/100 ft^2, HPHT FL 11.5 mL at 180 °C after 16 h aging — performance comparable to or exceeding the commercial modified starch (CMS) benchmark.

The Herschel–Bulkley model consistently provided the best fit ($R^2 \geq 0.997$) for all freshwater AMPS-modified mud formulations, significantly superior to Bingham Plastic and Power Law models.

A non-monotonic concentration dependence was observed, with AMPS-3.0 showing lower performance than AMPS-2.0, attributable to the over-treatment effect of excess free polymer chains competing with adsorbed chains for clay surface sites and reducing effective network connectivity at supra-optimal dosage.

The findings confirm that acid modification is a simple, scalable, and cost-effective route to improved starch-based WBDM additives suitable for moderate HTHP applications (up to 180 °C) and establish AMPS as a competitive green alternative to commercial modified starch products, with potential for further performance enhancement in salt-contaminated muds, through dual modification combining acid hydrolysis with crosslinking or graft copolymerization.

Nomenclatures

- %- percentage
- AMPS- Acid modified potato starch
- BT- bentonite
- C- carbon
- CMS- commercially modified starch
- DLS- dynamic light scattering
- DW- distilled water
- SEM- scanning electron microscropy
- FL- fluid loss
- FTIR- fourier transform infrared
- g-gram
- H- hydrogen
- HCL- hydrochloride
- HD- hydrodynamic diameters
- HTHP- high temperature high pressure
- HS- high salinity
- kJ mol^{-1} – kilojoules per mole
- mg g^{-1}- milligram per gram
- Mg- magnesium
- MgL^{-1}- milligram per litre
- mL- milli litres
- N- nitrogen
- Na- sodium
- NaLS- sodium lignosulfonate
- NC- nanocomposite
- Nm- nanometre
- OH - hydroxyl
- PD- Peak Diameter
- PDI- Polydispersity index
- S- sulphur
- SD- Standard deviation
- SEM- scanning electron microscopy
- Si- silicon
- WBDM- Water-based drilling mud
- TGA- thermogravimetric analysis
- Zn- zinc

Compliance with ethical standards

Acknowledgments

The authors would like to acknowledge the financial support from Universiti Teknologi Malaysia for 13 the funding under UTM Fundamental Research Grant (UTMFR) (Q.J130000.3846.23H10) and UTM Collaborative Research Grant (Q.J130000.3046.10G31).

Disclosure of conflict of interest

The authors declare that they have no known competing financial interests or personal relationships that could have appeared to influence the work reported in this paper.

Data availability

The datasets generated during and/or analysed during the current study are available from the corresponding author on reasonable request.

CRediT authorship contribution statement

Samuelson I. Okwaraku; Inyeaka Hanachor; Writing – review & editing, Validation, Software, Methodology, Formal analysis, Data curation, Conceptualization. **Allison D. Natuke; Sonia Shialong**: Validation, Supervision, Resources, Project administration. **Sonia Shialong:** Visualization, Methodology, Investigation. **Obamanu Tamunotonjo; Ogunwole B. Olalekan:** Writing – review & editing, Formal analysis, Data curation.

References

[1] Antia, M., et al., *Environmental and public health effects of spent drilling fluid: an updated systematic review.* Journal of Hazardous Materials Advances, 2022. **7**: p. 100120.

[2] Davoodi, S., et al., *Modified-starch applications as fluid-loss reducers in water-based drilling fluids: A review of recent advances.* Journal of cleaner production, 2024. **434**: p. 140430.

[3] Wu, X., et al. *Preparation and Application of Environmentally-Friendly Copolymer Filtration Control Agent Based on Hydrogen Bonding*. in *Journal of Physics: Conference Series*. 2024. IOP Publishing.

[4] You, F., Y. Zheng, and X. Gong, *Filtration control properties of four native starches in water-based drilling fluids.* International Journal of Biological Macromolecules, 2024. **283**: p. 137580.

[5] Ali, J.A., et al., *Application of ultra-fine particles of potato as eco-friendly green additives for drilling a borehole: A filtration, rheological and morphological evaluation.* Chemical Engineering Research and Design, 2024. **206**: p. 89-107.

[6] Assi, A.H., *Potato starch for enhancing the properties of the drilling fluids.* Iraqi Journal of Chemical and Petroleum Engineering, 2018. **19**(3): p. 33-40.

[7] Ali, I., M. Ahmad, and T. Ganat, *Experimental investigation of rheological and filtration behavior of water-based mud using response surface methodology (RSM).* Solid State Technol, 2020. **63**: p. 1240-1251.

[8] Wang, B., J. Liu, and Z. Song, *Eco-Friendly Filtrate Control in Drilling Fluids: Itaconic Acid-Grafted Corn Starch from Natural Organic Materials with Thermal and Salt/Calcium Resistance.* Polymers, 2026. **18**(2): p. 244.

[9] Ali, I., M. Ahmad, and N. Lashari, *Optimizing filtration properties of water based drilling mud systems using dually modified starch.* Journal of Cleaner Production, 2024. **454**: p. 142022.

[10] Tong, C., et al., *Toward an understanding of potato starch structure, function, biosynthesis, and applications.* Food Frontiers, 2023. **4**(3): p. 980-1000.

[11] Al-Hameedi, A.T., et al., *Proposing a new biodegradable thinner and fluid loss control agent for water-based drilling fluid applications.* International Journal of Environmental Science and Technology, 2020. **17**(8): p. 3621-3632.

[12] Ebuzeme, I., O. Olatunji, and B. Olufemi. *Factorial Design Validation of an Environmentally Benign Water-Based Drilling Fluid from Sweet Potato Peels at Elevated Temperatures*. in *SPE Nigeria Annual International Conference and Exhibition*. 2021. SPE.

[13] Sid, A.N.E.H., et al., *The Synergistic Effect of Algerian Na-Bentonite/Potato Starch/Grass Powder on the Enhancement of Aged Water-based Drilling Fluids.* Arabian Journal for Science and Engineering, 2022. **47**(9): p. 11721-11732.

[14] Xie, Q., et al., *A comprehensive review of starch: Structure, properties, chemical modification, and application in food preservation.* Food Frontiers, 2025. **6**(4): p. 1645-1657.

[15] Dai, L., J. Zhang, and F. Cheng, *Succeeded starch nanocrystals preparation combining heat-moisture treatment with acid hydrolysis.* Food Chemistry, 2019. **278**: p. 350-356.

[16] Singh, V. and S. Ali, *Properties of starches modified by different acids.* International Journal of Food Properties, 2008. **11**(3): p. 495-507.

[17] Li, S., et al., *Enzymatic chain elongation of A-, B-, and C-type grain starches by amylosucrase: Universal structure–function rules for resistant-starch design.* Food Research International, 2025: p. 118135.

[18] Song, H.-g., et al., *Comparative study on physicochemical properties of starch films prepared from five sweet potato (Ipomoea batatas) cultivars.* International Journal of Biological Macromolecules, 2021. **189**: p. 758-767.

[19] Nakamura, Y., et al., *The relationship between the fine structure of amylopectin and the type of crystalline allomorph of starch granules in rice endosperm.* Cereal Chemistry, 2023. **100**(3): p. 721-733.

[20] Varghese, S., et al., *Amylose–amylopectin ratio: Comprehensive understanding of structure, physicochemical attributes, and applications of starch*, in *Handbook of biopolymers*. 2022, Springer. p. 1-30.

[21] Jiang, H. and J.-L. Jane, *Chemical and Physical Structures of Starch*, in *Handbook of Starch Science and Technology*. 2025, CRC Press. p. 112-123.

[22] Jiang, X., et al., *Synthesis and formation mechanism of amorphous silica particles via sol–gel process with tetraethylorthosilicate.* Ceramics International, 2019. **45**(6): p. 7673-7680.

[23] Guo, C., et al., *Effect of sulfuric acid hydrolysis on the structure and Pickering emulsifying capacity of acorn starch.* Food Chemistry: X, 2024. **22**: p. 101277.

[24] Makowska, A., et al., *Polymer-Solvent Interactions in Modified Starches Pastes-Electrokinetic, Dynamic Light Scattering, Rheological and Low Field Nuclear Magnetic Resonance Approach.* Polymers (Basel), 2022. **14**(15).

[25] Sujka, M. and A.E. Wiącek, *Physicochemical Characteristics of Porous Starch Obtained by Combined Physical and Enzymatic Methods, Part 1: Structure, Adsorption, and Functional Properties.* International Journal of Molecular Sciences, 2024. **25**(3): p. 1662.

[26] Omotioma, M., et al., *Effects of process factors on the characteristics of water based mud viscosified by kaolin and bentonite.* Read. Time, 2024. **192**: p. 04-09.

[27] Andriyko, L., et al., *The influence of the aqueous media acidity on the electrokinetic potential, aggregation and adsorption properties of silica nanoparticles synthesized from metallurgical wastes.* Journal of Molecular Liquids, 2023. **392**: p. 123513.

[28] Davoodi, S., et al., *Synthetic polymers: A review of applications in drilling fluids.* Petroleum Science, 2024. **21**(1): p. 475-518.

[29] Mansoori, Y., et al., *Polymer–clay nanocomposites: Free-radical grafting of polyacrylamide onto organophilic montmorillonite.* European Polymer Journal, 2010. **46**(9): p. 1844-1853.

[30] Okoro, E.E., et al., *Performance evaluation of chemically modified starch-based additives for enhanced water-based mud formulations in high-temperature and salinity drilling operations.* Polymer Bulletin, 2025. **82**(13): p. 8115-8145.

[31] Abdollahi, M., A. Varamesh, and A. Nasiri, *Improvement in the performance of potato starch used in the water-based drilling fluid via its chemical modification by grafting copolymerization.* Science and Technology, 2009. **22**(4): p. 251-260.

[32] Chu, T., et al., *Development of high strength potato starch nanocomposite films with excellent UV-blocking performance: Effect of heat moisture treatment synergistic with ligninsulfonic acid.* Industrial Crops and Products, 2022. **187**: p. 115327.

[33] Ali, I., M. Ahmad, and T. Ganat, *Biopolymeric formulations for filtrate control applications in water-based drilling muds: A review.* Journal of Petroleum Science and Engineering, 2022. **210**: p. 110021.